radiation, Oriental Yeast Co., Japan). Five rats per group were administered with phorone (40, 120 or 400 mg/kg, i.p.). Five rats per group were administered orally with acetaminophen (1000 mg/kg), bromobenzene (300 mg/kg), clofibrate (300 mg/kg), chlorpromazine (45 mg/kg), glibenclamide (1000 mg/kg), methapyrilene (100 mg/kg), phenylbutazone (200 mg/kg), aspirin (450 mg/kg), carbon tetrachloride (300 mg/kg), coumarin (150 mg/kg), hexachlorobenzene (300 mg/kg), perhexiline maleate (150 mg/kg) or thioacetamide (45 mg/kg). Blood samples were collected in tubes containing heparin lithium 3, 6, 9, or 24 hr after treatment for biochemical assay. The animals were then euthanized and the liver was removed and soaked in RNA*later* (Ambion, Austin, TX, USA) immediately after sampling and stored at –80°C until use for gene expression analysis. In the animals treated with phorone or bromobenzene, another aliquot of liver sample was immediately frozen in liquid nitrogen for measurement of hepatic glutathione contents. The remaining liver samples were then removed and fixed in 10% neutral buffered formalin for histopathological examination. The experimental protocol was reviewed and approved by the Ethics Review Committee for Animal Experimentation of the National Institute of Health Sciences.

Plasma biochemistry

Activities of alanine aminotransferase (ALT) and aspartate aminotransferase (AST) in plasma were determined using a 7080 Clinical Analyzer (Hitachi High-Technologies Corporation, Tokyo, Japan).

Histopathology

The fixed samples were dehydrated through graded alcohols and embedded in paraffin. Serial sections 2-3 μm thick were stained with hematoxylin and eosin for pathological examination.

Measurement of hepatic glutathione content

The liver samples (0.1 g) were homogenized with 5% 5-sulfosalicylic acid (Sigma-Aldrich) and centrifuged at 12,000 rpm for 10 min at 4°C. The supernatant was used for the measurement of total glutathione content in the liver using theTotal Glutathione Quantification Kit (Dojindo Laboratories), according to the manufacturer's instructions.

Microarray analysis

Liver samples were homogenized with RLT buffer, supplied in the RNeasy Mini Kit (Qiagen, Valencia, CA, USA), using Mill Mixer (Qiagen) and zirconium beads. Total RNA was isolated using Bio Robot 3000 (Qiagen). DNase I treatment was performed using RNase-Free DNase set (Qiagen) for 15 min at room temperature. GeneChip analysis was performed on 3 out of 5 samples in each group according to the Affymetrix standard protocol. Briefly, a total of RNA of 5 μg prepared from the individual rat liver samples was used for cDNA synthesis using the T7-$(dT)_{24}$ primer (Affymetrix) and Superscript Choice System (Invitrogen, Carlsbad, CA, USA). The cDNA was purified using cDNA Cleanup Module (Affymetrix), and biotin-labeled cRNA mix was transcribed using the BioArray High Yield RNA Transcription Labeling Kit (Enzo Diagnostics, Farmingdale, NY, USA). Ten micrograms of fragmented cRNA cocktails were hybridized to the RAE 230A GeneChip array for all samples except for that of phorone- and corresponding vehicle-treated rats, which were hybridized to the RAE 230 2.0 array for 18 hr at 45°C at 60 rpm. GeneChip was washed and stained using Fluidics Station 400 (Affymetrix) according to the Affymetrix standard protocol and scanned using Gene Array Scanner (Affymetrix). The scanned data images were digitalized using Affymetrix Microarray Suite ver. 5.0 (Affymetrix), and the data was scaled by adjusting the mean Signal value to 500.

Microarray data analysis

We primarily use gloval mean normalization for data analysis in our project. Firstly, using vehicle- and phorone (40 and 120 mg/kg)-treated rats, where the total number of rats was 36, both Spearman's and Pearson's correlation coefficients between the signal value and hepatic glutathione content were calculated for all the probe sets that existed on the RAE 230A array. The probe sets with both Spearman's coefficients and Pearson's coefficients less than -0.329 were chosen as statistically significant inverse correlations ($N=36$, $p < 0.05$). Secondly, probe sets, whose average signal values in 120 mg/kg phorone-treated rats at 3 h were above 1.5 compared to those of corresponding controls were selected. Then, probe sets, whose detection calls determined by Microarray Suite ver. 5.0 were all present 3 hr after phorone treatment, were selected. Finally, annotation for each probe set was obtained using NetAffx Website (Liu *et al.*, 2003), and probe sets without unique Entrez Gene ID were excluded from the analysis. For each probe set, the signal data was z-score normalized in the vehicle- and phorone (40, 120 and 400 mg/kg)-treated group. All the z-score

normalized signal data were presented as a heat map and z-score normalized glutathione content data was also presented as a heat map.

Statistical analysis

Dunnett's test was performed for serum chemistry and glutathione content data (between phorone-treated rat groups and vehicle-treated group at the same time point), using R software (www.r-project.org). Serum chemistry data (other than that of phorone-treated rats) was analyzed by F-test to evaluate the homogeneity of variance. If the variance was homogeneous, Student's *t*-test was applied. If the variance was heterogeneous, Aspin-Welch's *t*-test was performed (Snedecor and Cochran, 1989). F-test, Student's *t*-test and Aspin-Welch's *t*-test were performed using Microsoft Excel 2007. Both Spearman's and Pearson's correlation coefficients were calculated using Microsoft Excel 2007. A p-value of < 0.05 was considered statistically significant. Principal component analysis (PCA) was performed using the Spotfire Functional Genomics Package ver. 17.4.832 (Spotfire, Somerville, MA, USA).

RESULTS

Plasma biochemistry in phorone-treated rats

There were no apparent fluctuations of plasma ALT activity in 40 and 120 mg/kg phorone-treated rats throughout the experimental period (Fig. 1). Plasma ALT activity was obviously elevated in rats 24 hr after 400 mg/kg phorone treatment.

Glutathione content in phorone-treated rat liver

Hepatic glutathione content was significantly decreased 3, 6 and 9 hr for 40 mg/kg phorone-treated rats, and recovered above the control level 24 hr after treatment (Fig. 2). Hepatic glutathione content was significantly decreased to an 8.3-fold lower level compared with the control 3 hr after the 120 mg/kg phorone-treated rats, and gradually recovered 6 and 9 hr after treatment, resulting in a 1.52-fold higher level compared with control 24 hr after treatment. Hepatic glutathione content was significantly decreased to a 22- to 30-fold lower level compared with control 3, 6 and 9 hr after the 400 mg/kg phorone-treated rats, and recovered to the control level 24 hr after treatment.

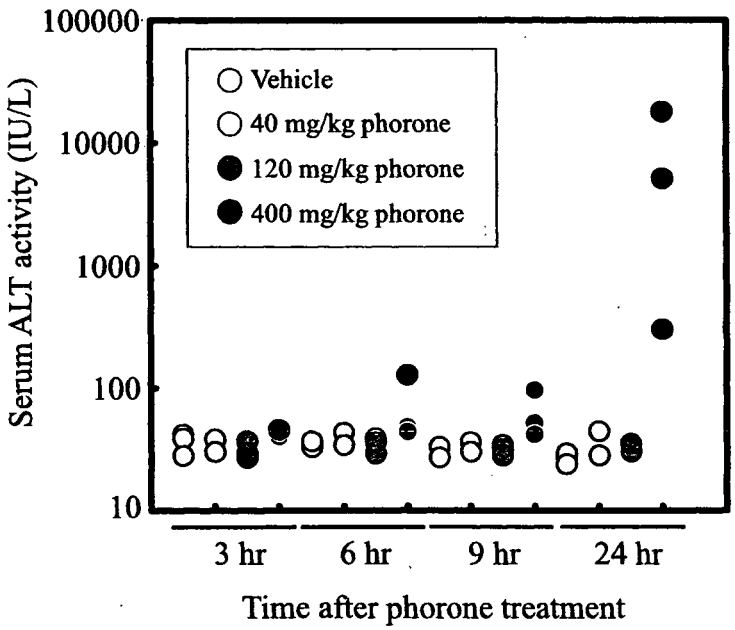

Fig. 1. Activity of alanine aminotransferase in plasma. Each dot represents the value of an individual animal.

Identification of glutathione deficiency-correlated gene probe sets

A hundred and sixty-one probe sets were identified as glutathione deficiency-correlated gene probe sets, or GSH probe sets (Table 1), and classified to 5 groups, i.e., "antioxidant, phase II drug metabolizing enzymes, and oxidative stress markers" (11 probe sets), "transporter" (13 probe sets), "metabolism" (20 probe sets), "transcription factors and signal transduction-related, and protein turnover-related genes" (79 probe sets), and "miscellaneous" (37 probe sets). Both the z-score transformed hepatic glutathione content and z-score transformed signal levels of the GSH probe sets are presented as a heat map (Fig. 3). PCR primers and TaqMan probes for 4 genes from the list above, namely tribbles homolog 3 (accession no. AB020967), heme oxygenase-1 (NM_012580), thioredoxin reductase-1 (NM_031614) and γ-glutamylcysteine synthetase modifier subunit (NM_017305), were synthesized and quantitative RT-PCR was performed using the TaqMan Universal PCR Master Mix (Applied Biosystems), and the mRNA level was quantified with a GeneAmp 5700 Sequence Detection System (Applied Biosystems) according to the manufacturer's instructions. It was confirmed that quantification by GeneChip was sufficient (data not shown).

Plasma biochemistry and histopathological findings in rat liver treated with various hepatotoxicants

Rats treated with bromobenzene, methapyrilene or thioacetamide showed significant increase in plasma ALT activity 24 hr after treatment (Table 2). Rats treated with acetaminophen, chlorpromazine, glibenclamide or methapyrilene showed significant increase in serum AST activity 24 hr after treatment. Rats treated with acetaminophen, bromobenzene, methapyrilene, carbon tetrachloride, coumarin or thioacetamide showed histopathological changes 24 hr after treatment, while rats treated with clofibrate, chlorpromazine, glibenclamide, phenylbutazone, aspirin,

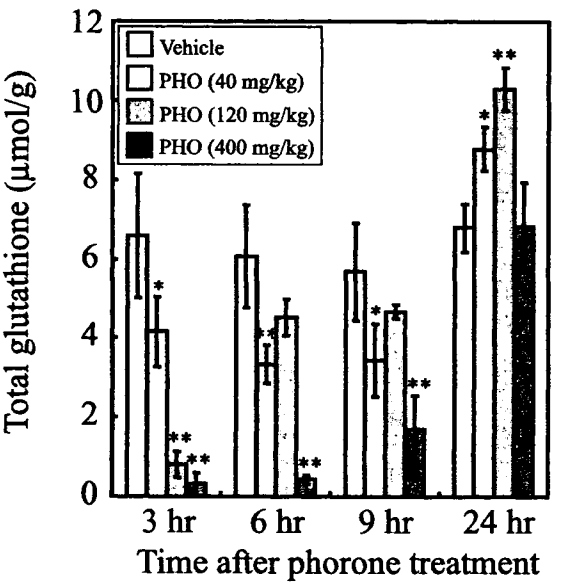

Fig. 2. Hepatic glutathione content after phorone treatment.
Three rats per group were treated with 40, 120 or 400 mg/kg phorone or vehicle, and the livers were removed 3, 6, 9 and 24 hr after treatment. Hepatic glutathione content (total) was measured and the data are presented as mean ± S.D. ** and *, $p<0.01$ and $p<0.05$ by Dunnett's test, respectively.

Table 1. Glutathione depletion-responsive gene probe sets (GSH probe sets).

Affymetrix probe ID	Correlation coefficient		Gene Symbol	Annotation
	Spearman's	Pearson's		
Antioxidant, phase II drug-metabolizing enzymes and oxidative stress markers				
1368037_at	−0.602	−0.368	Cbr1	carbonyl reductase 1
1387221_at	−0.720	−0.712	Gch	GTP cyclohydrolase 1
1368503_at	−0.702	−0.650	Gch	GTP cyclohydrolase 1
1370030_at	−0.570	−0.448	Gclm	glutamate cysteine ligase, modifier subunit
1370080_at	−0.611	−0.609	Hmox1	heme oxygenase (decycling) 1
1387282_at	−0.680	−0.589	Hspb8	heat shock 22kDa protein 8
1388721_at	−0.747	−0.660	Hspb8	heat shock 22kDa protein 8
1389578_at	−0.649	−0.582	Isrip	ischemia/reperfusion inducible protein
1372510_at	−0.589	−0.578	Srxn1	Sulfiredoxin 1 homolog (S. cerevisiae)
1398791_at	−0.600	−0.471	Txnrd1	thioredoxin reductase 1
1386958_at	−0.666	−0.459	Txnrd1	thioredoxin reductase 1
Transporter				
1374423_at	−0.711	−0.688	Hiat1_predicted	hippocampus abundant gene transcript 1 (predicted)
1370934_at	−0.656	−0.579	Nup153	nucleoporin 153
1367803_at	−0.430	−0.523	Nup54	nucleoporin 54
1371754_at	−0.330	−0.497	Slc25a25	solute carrier family 25 (mitochondrial carrier, phosphate carrier), member 25
1369099_at	−0.356	−0.567	Slc30a1	solute carrier family 30 (zinc transporter), member 1
1370286_at	−0.858	−0.813	Slc38a2	solute carrier family 38, member 2
1398771_at	−0.651	−0.520	Slc3a2	solute carrier family 3 (activators of dibasic and neutral amino acid transport), member 2
1387130_at	−0.726	−0.455	Slc40a1	solute carrier family 39 (iron-regulated transporter), member 1
1387693_a_at	−0.731	−0.601	Slc6a9	solute carrier family 6 (neurotransmitter transporter, glycine), member 9
1369772_at	−0.609	−0.473	Slc6a9	solute carrier family 6 (neurotransmitter transporter, glycine), member 9
1373787_at	−0.619	−0.513	Slc6a9	solute carrier family 6 (neurotransmitter transporter, glycine), member 9
1368391_at	−0.780	−0.700	Slc7a1	solute carrier family 7 (cationic amino acid transporter, y^+ system), member 1
1368392_at	−0.591	−0.626	Slc7a1	solute carrier family 7 (cationic amino acid transporter, y^+ system), member 1
Metabolism				
1387925_at	−0.747	−0.574	Asns	asparagine synthetase
1386928_at	−0.352	−0.409	Bcat2	branched chain aminotransferase 2, mitochondrial
1374034_at	−0.762	−0.756	Cars_predicted	cysteinyl-tRNA synthetase (predicted)
1368709_at	−0.537	−0.492	Fut1	fucosyltransferase 1
1375852_at	−0.441	−0.532	Hmgcr	3-hydroxy-3-methylglutaryl-Coenzyme A reductase
1387848_at	−0.413	−0.500	Hmgcr	3-hydroxy-3-methylglutaryl-Coenzyme A reductase
1376418_a_at	−0.679	−0.549	Iars_predicted	isoleucine-tRNA synthetase (predicted)

Table 1. Continued.

Affymetrix probe ID	Correlation coefficient		Gene Symbol	Annotation
	Spearman's	Pearson's		
1389551_at	–0.373	–0.359	Lactb2	lactamase, beta 2
1371350_at	–0.773	–0.683	LOC683283	similar to S-adenosylmethionine synthetase isoform type-2 (Methionine adenosyltransferase 2) (AdoMet synthetase 2) (Methionine adenosyltransferase II) (MAT-II)
1377287_at	–0.495	–0.532	Mars2_predicted	methionine-tRNA synthetase 2 (mitochondrial) (predicted)
1375684_at	–0.554	–0.490	Neu1	neuraminidase 1
1367811_at	–0.675	–0.459	Phgdh	3-phosphoglycerate dehydrogenase
1369785_at	–0.754	–0.691	Ppat	phosphoribosyl pyrophosphate amidotransferase
1388756_at	–0.614	–0.529	Ppcs	phosphopantothenoylcysteine synthetase
1372665_at	–0.682	–0.633	Psat1	phosphoserine aminotransferase 1
1375964_at	–0.641	–0.615	Psph	phosphoserine phosphatase
1388521_at	–0.428	–0.544	Pycs_predicted	pyrroline-5-carboxylate synthetase (glutamate gamma-semialdehyde synthetase) (predicted)
1372602_at	–0.490	–0.460	RGD1311800	similar to genethonin 1
1398452_at	–0.421	–0.431	RGD1559923_predicted	similar to chromosome 14 open reading frame 35 (predicted)
1372009_at	–0.569	–0.478	Yars	tyrosyl-tRNA synthetase
Transcription factor, signal transduction-related and protein turnover-related gene				
1388179_at	–0.370	–0.379	Acvr2b	activin receptor IIB
1369146_a_at	–0.433	–0.479	Ahr	aryl hydrocarbon receptor
1378140_at	–0.600	–0.606	Arl11	ADP-ribosylation factor-like 11
1367960_at	–0.470	–0.485	Arl4a	ADP-ribosylation factor-like 4A
1389623_at	–0.605	–0.623	Atf1	activating transcription factor 1
1375941_at	–0.594	–0.513	Baiap2l1	BAI1-associated protein 2-like 1
1374947_at	–0.584	–0.567	Bcar3_predicted	breast cancer anti-estrogen resistance 3 (predicted)
1376754_at	–0.771	–0.740	Cars_predicted	cysteinyl-tRNA synthetase (predicted)
1391572_at	–0.804	–0.802	Cars_predicted	cysteinyl-tRNA synthetase (predicted)
1387087_at	–0.720	–0.734	Cebpb	CCAAT/enhancer binding protein (C/EBP), beta
1387244_at	–0.504	–0.371	Cgrrf1	cell growth regulator with ring finger domain 1
1372498_at	–0.626	–0.608	Ciapin1	cytokine induced apoptosis inhibitor 1
1399141_at	–0.640	–0.664	Clk4	CDC like kinase 4
1376811_a_at	–0.571	–0.534	Cpsf6_predicted	cleavage and polyadenylation specific factor 6, 68kDa (predicted)
1369737_at	–0.558	–0.614	Crem	cAMP responsive element modulator
1370979_at	–0.433	–0.475	Ddx20	DEAD/H (Asp-Glu-Ala-Asp/His) box polypeptide 20, 103kD
1375901_at	–0.497	–0.360	Ddx21a	DEAD (Asp-Glu-Ala-Asp) box polypeptide 21a
1373200_at	–0.581	–0.505	Eef1e1_predicted	eukaryotic translation elongation factor 1 epsilon 1 (predicted)

Table 1. Continued.

Affymetrix probe ID	Correlation coefficient		Gene Symbol	Annotation
	Spearman's	Pearson's		
1368967_at	–0.629	–0.484	Eif2b3	eukaryotic translation initiation factor 2B, subunit 3 gamma
1386888_at	–0.794	–0.776	Eif4ebp1	eukaryotic translation initiation factor 4E binding protein 1
1388666_at	–0.581	–0.588	Encl	ectodermal-neural cortex 1
1382059_at	–0.593	–0.634	Fbxo30	F-box protein 30
1372526_at	–0.675	–0.776	Flcn	folliculin
1374530_at	–0.671	–0.601	Fzd7_predicted	frizzled homolog 7 (Drosophila) (predicted)
1373499_at	–0.731	–0.622	Gas5	growth arrest specific 5
1388953_at	–0.682	–0.665	Gnl3	guanine nucleotide binding protein-like 3 (nucleolar)
1373094_at	–0.788	–0.587	Gtf2h1_predicted	general transcription factor II H, polypeptide 1 (predicted)
1367741_at	–0.618	–0.579	Herpud1	homocysteine-inducible, endoplasmic reticulum stress-inducible, ubiquitin-like domain member 1
1372693_at	–0.462	–0.559	Hnrpa1	heterogeneous nuclear ribonucleoprotein A1
1387430_at	–0.754	–0.774	Hsf2	heat shock factor 2
1388587_at	–0.571	–0.636	Ier3	immediate early response 3
1367795_at	–0.666	–0.597	Ifrd1	interferon-related developmental regulator 1
1368160_at	–0.644	–0.700	Igfbp1	insulin-like growth factor binding protein 1
1387440_at	–0.432	–0.330	Ireb2	iron responsive element binding protein 2
1373374_at	–0.813	–0.812	Lmo4	LIM domain only 4
1373303_at	–0.339	–0.409	LOC312030	similar to splicing factor, arginine/serine-rich 2, interacting protein
1374154_at	–0.762	–0.677	LOC312030	Similar to splicing factor, arginine/serine-rich 2, interacting protein
1374857_at	–0.555	–0.445	LOC499709	similar to nucleolar protein family A, member 1
1373133_at	–0.630	–0.692	LOC500282	similar to ADP-ribosylation factor-like 10C
1368874_a_at	–0.775	–0.801	Mafg	v-maf musculoaponeurotic fibrosarcoma oncogene family, protein G (avian)
1368273_at	–0.342	–0.453	Mapk6	mitogen-activated protein kinase 6
1384427_at	–0.766	–0.764	Mdm2_predicted	transformed mouse 3T3 cell double minute 2 homolog (mouse) (predicted)
1388990_at	–0.544	–0.492	Mki67ip	Mki67 (FHA domain) interacting nucleolar phosphoprotein
1375442_at	–0.670	–0.696	Mphosph10_predicted	M-phase phosphoprotein 10 (U3 small nucleolar ribonucleoprotein) (predicted)
1368308_at	–0.513	–0.622	Myc	myelocytomatosis viral oncogene homolog (avian)
1374437_at	–0.717	–0.665	Nars	asparaginyl-tRNA synthetase
1376704_a_at	–0.577	–0.485	Ndnl2	necdin-like 2
1389996_at	–0.645	–0.657	Nek1_predicted	NIMA (never in mitosis gene a)-related expressed kinase 1 (predicted)
1389765_at	–0.564	–0.579	Nle1_predicted	notchless homolog 1 (Drosophila) (predicted)
1368173_at	–0.444	–0.403	Nol5	nucleolar protein 5
1368032_at	–0.451	–0.365	Nolc1	nucleolar and coiled-body phosphoprotein 1
1387152_at	–0.375	–0.508	Nrbf2	nuclear receptor binding factor 2

Table 1. Continued.

Affymetrix probe ID	Correlation coefficient		Gene Symbol	Annotation
	Spearman's	Pearson's		
1368068_a_at	–0.605	–0.488	Pacsin2	protein kinase C and casein kinase substrate in neurons 2
1372857_at	–0.720	–0.706	Pacsin2	protein kinase C and casein kinase substrate in neurons 2
1374326_at	–0.576	–0.544	Ppan	peter pan homolog (Drosophila)
1369104_at	–0.618	–0.554	Prkaa1	protein kinase, AMP-activated, alpha 1 catalytic subunit
1368087_a_at	–0.419	–0.407	Ptpn21	protein tyrosine phosphatase, non-receptor type 21
1371081_at	–0.740	–0.765	Rapgef4	Rap guanine nucleotide exchange factor (GEF) 4
1374750_at	–0.773	–0.799	Rapgef6_predicted	Rap guanine nucleotide exchange factor (GEF) 6 (predicted)
1388522_at	–0.689	–0.713	RGD1310383_predicted	similar to T-cell activation protein phosphatase 2C (predicted)
1374945_at	–0.587	–0.463	RGD1359191	GCD14/PCMT domain containing protein RGD1359191
1373075_at	–0.762	–0.664	RGD1560888_predicted	similar to Cell division protein kinase 8 (Protein kinase K35) (predicted)
1372062_at	–0.703	–0.708	RGD1563395_predicted	similar to cyclin-dependent kinase 2-interacting protein (predicted)
1371517_at	–0.660	–0.627	RGD1566234_predicted	similar to Grb10 protein (predicted)
1377503_at	–0.558	–0.606	Riok2	RIO kinase 2 (yeast)
1387201_at	–0.766	–0.774	Rnf138	ring finger protein 138
1389258_at	–0.592	–0.653	Rnf138	ring finger protein 138
1376440_at	–0.741	–0.715	Rnf139_predicted	ring finger protein 139 (predicted)
1398572_at	–0.670	–0.547	Rnmt	RNA (guanine-7-) methyltransferase
1376065_at	–0.662	–0.617	Rrs1_predicted	RRS1 ribosome biogenesis regulator homolog (S. cerevisiae) (predicted)
1375441_at	–0.724	–0.680	Sars1	seryl-aminoacyl-tRNA synthetase 1
1374864_at	–0.370	–0.339	Spry2	sprouty homolog 2 (Drosophila)
1388967_at	–0.744	–0.714	Tcfe3_predicted	transcription factor E3 (predicted)
1388780_at	–0.683	–0.681	Terf2ip	telomeric repeat binding factor 2, interacting protein
1387450_at	–0.695	–0.708	Tgfa	transforming growth factor alpha
1370694_at	–0.858	–0.760	Trib3	tribbles homolog 3 (Drosophila)
1386321_s_at	–0.835	–0.676	Trib3	tribbles homolog 3 (Drosophila)
1370695_s_at	–0.831	–0.701	Trib3	tribbles homolog 3 (Drosophila)
1388868_at	–0.779	–0.736	Zfp216_predicted	zinc finger protein 216 (predicted)
Miscellaneous				
1385616_a_at	–0.734	–0.557	Asf1a_predicted	ASF1 anti-silencing function 1 homolog A (S. cerevisiae) (predicted)
1389569_at	–0.647	–0.578	Bxdc2	brix domain containing 2
1373196_at	–0.378	–0.414	Efha2	EF hand domain family, member A2
1372873_at	–0.599	–0.673	Fbxo38_predicted	F-box protein 38 (predicted)
1373836_at	–0.412	–0.503	Fyttd1	Forty-two-three domain containing 1
1374043_at	–0.379	–0.444	Gramd3	GRAM domain containing 3

Table 1. Continued.

Affymetrix probe ID	Correlation coefficient		Gene Symbol	Annotation
	Spearman's	Pearson's		
1390208_at	–0.586	–0.522	Htatip2_predicted	HIV-1 tat interactive protein 2, homolog (human) (predicted)
1371995_at	–0.802	–0.762	Klhl21_predicted	kelch-like 21 (Drosophila) (predicted)
1374879_x_at	–0.525	–0.490	Larp5_predicted	La ribonucleoprotein domain family, member 5 (predicted)
1388709_at	–0.683	–0.558	LOC362703	similar to WD-repeat protein 43
1384101_at	–0.682	–0.722	LOC682507	similar to Neural Wiskott-Aldrich syndrome protein (N-WASP)
1373761_at	–0.530	–0.535	LOC686611	similar to Protein FAM60A (Tera protein)
1373282_at	–0.596	–0.503	LOC686808	similar to mitochondrial carrier protein MGC4399
1372869_at	–0.554	–0.510	LOC689842	similar to Nucleolar GTP-binding protein 1 (Chronic renal failure gene protein) (GTP-binding protein NGB)
1373904_at	–0.749	–0.702	Lysmd2_predicted	LysM, putative peptidoglycan-binding, domain containing 2 (predicted)
1393239_at	–0.349	–0.462	Mtfr1_predicted	Mitochondrial fission regulator 1 (predicted)
1387950_at	–0.644	–0.629	Nip7	nuclear import 7 homolog (S. cerevisiae)
1373445_at	–0.732	–0.645	Nol8_predicted	nucleolar protein 8 (predicted)
1373737_at	–0.664	–0.674	ORF19	open reading frame 19
1376118_at	–0.603	–0.543	Otub2_predicted	OTU domain, ubiquitin aldehyde binding 2 (predicted)
1374438_at	–0.447	–0.460	Otud4	OTU domain containing 4
1374612_at	–0.669	–0.585	Papd5_predicted	PAP associated domain containing 5 (predicted)
1388355_at	–0.751	–0.650	Rbm17	RNA binding motif protein 17
1389065_at	–0.458	–0.498	Rbm34	RNA binding motif protein 34
1389228_at	–0.685	–0.607	RGD1304825_predicted	similar to RIKEN cDNA 2010309E21 (predicted)
1372185_at	–0.621	–0.634	RGD1306582	similar to RIKEN cDNA 2610205E22
1390392_at	–0.754	–0.718	RGD1309602_predicted	similar to RIKEN cDNA 2500001K11 (predicted)
1372329_at	–0.657	–0.627	RGD1311435	similar to hypothetical protein PRO0971
1373049_at	–0.492	–0.490	RGD1562136_predicted	similar to D1Ertd622e protein (predicted)
1388900_at	–0.719	–0.671	RGD1566118_predicted	RGD1566118 (predicted)
1372871_at	–0.717	–0.711	RGD735175	hypothetical protein MGC:72616
1375565_at	–0.513	–0.518	Timm22	translocase of inner mitochondrial membrane 22 homolog (yeast)
1390237_at	–0.573	–0.351	Timm8a	translocase of inner mitochondrial membrane 8 homolog a (yeast)
1373277_at	–0.624	–0.577	Tm2d3_predicted	TM2 domain containing 3 (predicted)
1374793_at	–0.518	–0.522	Wdr3_predicted	WD repeat domain 3 (predicted)
1371729_at	–0.473	–0.544	Ypel5	yippee-like 5 (Drosophila)
1390476_at	–0.740	–0.680	Zbtb39_predicted	Zinc finger and BTB domain containing 39 (predicted)
1373767_at	–0.634	–0.552	Zfand2a	zinc finger, AN1-type domain 2A

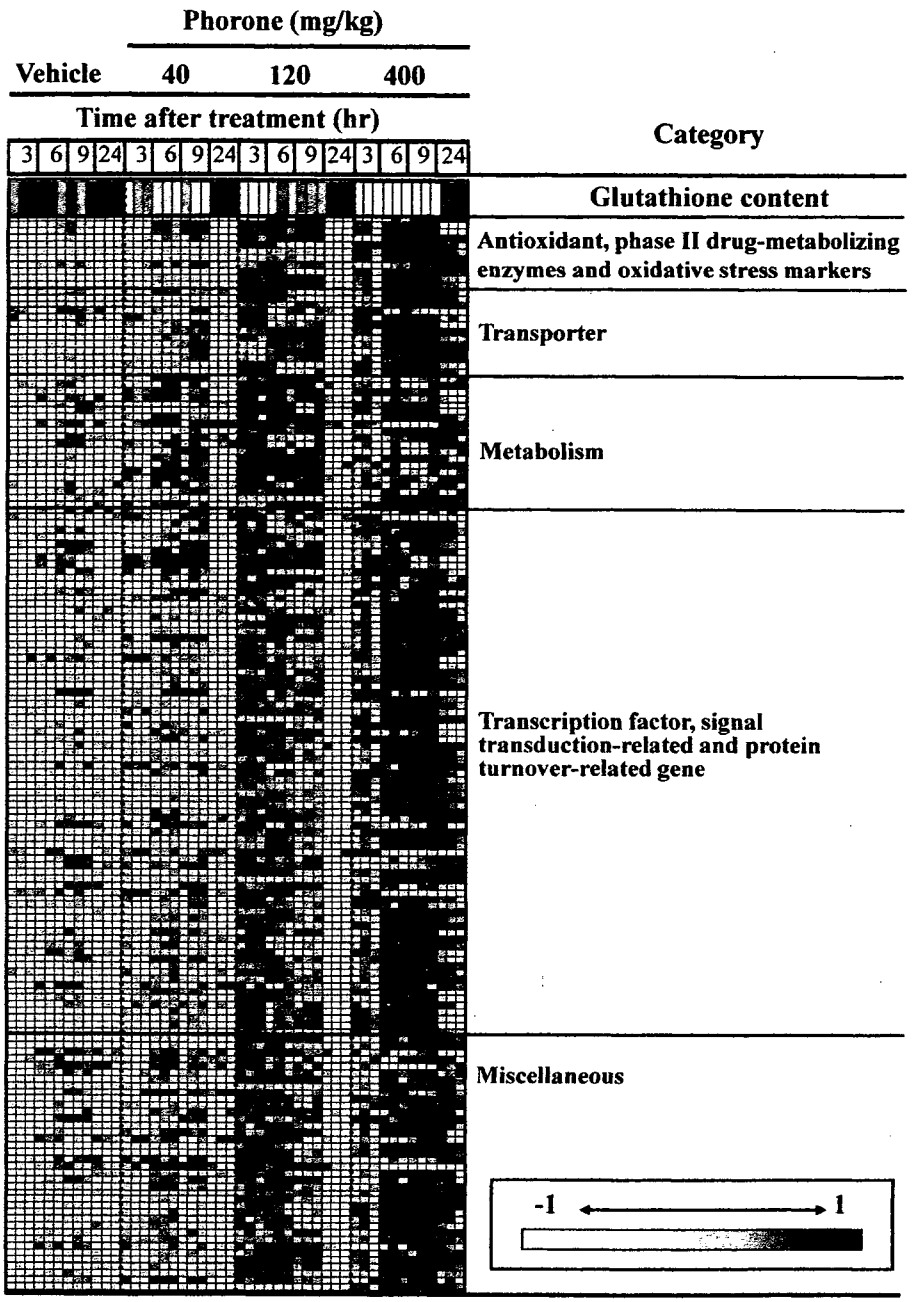

Fig. 3. Heat map representing glutathione content and gene expression level in rat liver treated with phorone.
Glutathione content and GeneChip signal data for GSH probe sets, obtained from rat livers treated with phorone or vehicle, are transformed to z-score by row, and are presented as a heat map where low and high scores are colored in white and black, respectively. Each row represents a probe set, and the vertical order of the probe sets is the same as that presented inTable 1. Each column represents individual rats treated either with phorone or vehicle.

Table 2. Plasma biochemistry and histopathological findings in rat liver treated with various prototypical hepatotoxicants.

Chemical	Dose (mg/kg)	Serum ALT activity (IU/L)		Serum AST activity (IU/L)		Histopathological findings observed in rat livers (number of animals)
		Control	Treated	Control	Treated	
Acetaminophen	1000	37.0 ± 3.1	51.0 ± 17.2	59.0 ± 6.3	76.4 ± 14.1*	Increased eosinophility of hepatocyte: central (3/5) Inflammatory infiltration: central (5/5)
Bromobenzene	300	50.8 ± 6.4	113.6 ± 49.9*	79.6 ± 7.0	481.0 ± 377.8	Hypertrophy, eosinophilic granular change (5/5) Cellular infiltration, centrilobular (5/5) Swelling, centrilobular (4/5) Necrosis, centrilobular (4/5)
Clofibrate	300	34.0 ± 5.5	38.0 ± 6.3	66.4 ± 8.0	79.0 ± 14.2	No findings
Chlorpromazine	45	32.4 ± 4.9	31.8 ± 1.8	62.2 ± 4.9	74.6 ± 8.4*	No findings
Glibenclamide	1000	32.2 ± 4.5	35.6 ± 2.9	61.4 ± 3.8	69.2 ± 4.7*	No findings
Methapyrilene	100	41.6 ± 9.5	68.4 ± 17.6*	71.8 ± 6.8	109.6 ± 25.7*	Single cell necrosis, hepatocyte (5/5) Hypertrophy, hepatocyte (5/5) Cellular infiltration, mononuclear cell, periportal (5/5) Anisoncleosis, hepatocyte (5/5)
Phenylbutazone	200	34.8 ± 4.8	49.4 ± 18.4	67.0 ± 6.3	76.6 ± 7.6	No findings
Aspirin	450	34.8 ± 5.3	44.2 ± 15.6	63.8 ± 4.5	75.6 ± 12.6	No findings
Carbon tetrachloride	300	37.2 ± 2.7	42.2 ± 4.6	66.6 ± 4.0	75.0 ± 13.3	Degeneration, hydropic: centrilobular (4/5) Cellular infiltration: centrilobular (3/5) Degeneration, fatty: centrilobular (4/5)
Coumarin	150	37.0 ± 3.9	40.2 ± 8.4	64.4 ± 8.6	85.8 ± 26.3	Hypertrophy, centrilobular (3/5)
Hexachlorobenzene	300	40.2 ± 8.7	47.0 ± 7.1	66.6 ± 3.3	69.2 ± 4.8	No findings
Perhexiline maleate	150	42.6 ± 5.9	50.0 ± 5.8	66.4 ± 5.1	71.6 ± 7.4	No findings
Thioacetamide	45	32.5 ± 3.4	137.2 ± 37.8**	63.5 ± 3.0	713.8 ± 542.6	Hypertrophy: centrilobular (5/5) Cellular infiltration, inflammatory (5/5) Change, eosinophilic hepatocyte (5/5) Necrosis, centrilobular (5/5)

Rat groups consisting of 5 animals were administered with the compounds listed in the table and euthanized 24 hr after treatment. Both blood chemistry and histopathology data are summarized using the 5 rats. Note that microarray analysis was conducted using 3 rats out of the 5. The data are presented as mean ±S.D. * and **, $p<0.05$ and $p<0.01$, respectively, determined by two-sample *t*-test.

hexachlorobenzene or perhexiline maleate did not show any histopathological changes.

Gene expression analysis for rat liver treated with various hepatotoxicants

PCA was performed using GSH probe sets for GeneChip data obtained from rat livers 24 hr after treatment with various prototypical hepatotoxicants (Fig. 4). It was obvious from the figure that a few compounds were distributed to the direction of the first principal component (PC 1) with relatively high contribution (57.6%), i.e., 300 mg/kg bromobenzene, 150 mg/kg coumarin, 1000 mg/kg acetaminophen, and 45 mg/kg thioacetamide, in that order. Rats treated with other chemicals or corresponding vehicles showed no apparent shift toward the PC 1 axis, but showed dispersed distributions along the PC 2 axis.

Glutathione content in rat livers treated with bromobenzene

From PCA using GSH probe sets, we found that bromobenzene was the most potent GSH-depletor among the compounds tested. In order to confirm this, hepatic glutathione content in the liver treated with this compound was actually quantified. It was found that the contents were significantly reduced 3, 6 and 9 hr after 300 mg/kg bromobenzene treatment (Fig. 5). It appeared that some of the treated rats showed recovery or rather rebound of GSH contents 24 hr after treatment since the mean value recovered to the control level with large variance.

Time-course of gene expression profile in rat liver treated with bromobenzene

In order to analyze the time dependent correlation between GSH contents and gene expression changes, PCA was performed by adding the data of 3, 6, and 9 hr after bromobenzene treatment to the same

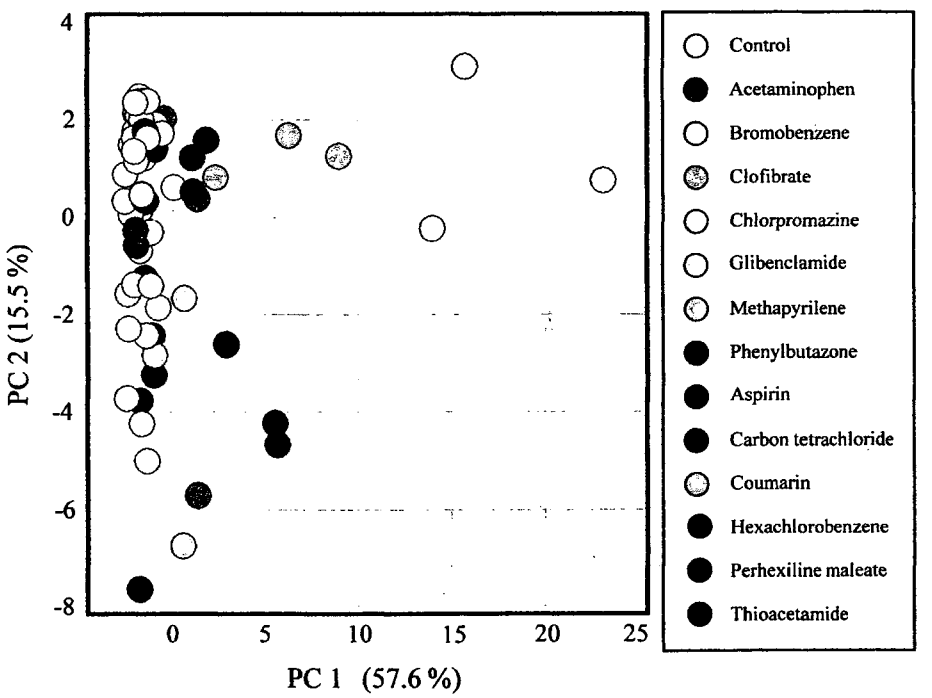

Fig. 4. PCA for GeneChip data of rat liver 24 hr after treatment with various hepatotoxicants. PCA was performed using GSH probe sets for GeneChip data of rat livers 24 hr after treatment with various hepatotoxicants. Each spot, colored by chemical type, represents individual samples. Bromobenzene, coumarin, and acetaminophen showed apparent shift from control, suggesting a perturbation of glutathione homeostasis in the liver after treatment.

data in Fig. 4. Fig. 6 shows that signal profiles of GSH probe sets did not apparently differ from those of controls, 3 and 6 hr after 300 mg/kg bromobenzene treatment. After 9 hr, they shifted away toward both PC1 and PC2 axis, approaching the position of 24 hr on PC1 axis.

DISCUSSION

Hepatic total glutathione content was significantly decreased in all the phorone-treated groups 3 hr after treatment (Fig. 2). After acute glutathione depletion, the hepatic glutathione content gradually recovered from 6 hr in the phorone-treated group (40 and 120 mg/kg), resulting in a significantly higher glutathione content, compared to the vehicle-treated rats 24 hr after treatment. Plasma ALT activity was elevated from 9 hr after 400 mg/kg phorone treatment, suggesting slight hepatocellular injury. Since secondary undesirable effects caused by slight hepatotoxicity (other than glutathione depletion) might affect the gene expression profile, we excluded GeneChip data of the 400 mg/kg phorone-treated rats from analysis for identification of the glutathione depletion-responsive gene probe sets. Previously, candidate marker genes whose mRNA levels were inversely correlated with hepatic glutathione content were identified using L-buthionine-[S,R]-sulfoximine (BSO) as a glutathione-depleting agent (Kiyosawa *et al.*, 2004). In the present study, we used phorone as a glutathione-depleting agent instead of BSO. We identified a total of 161 probe sets, referred to as 'GSH probe sets', whose signal showed

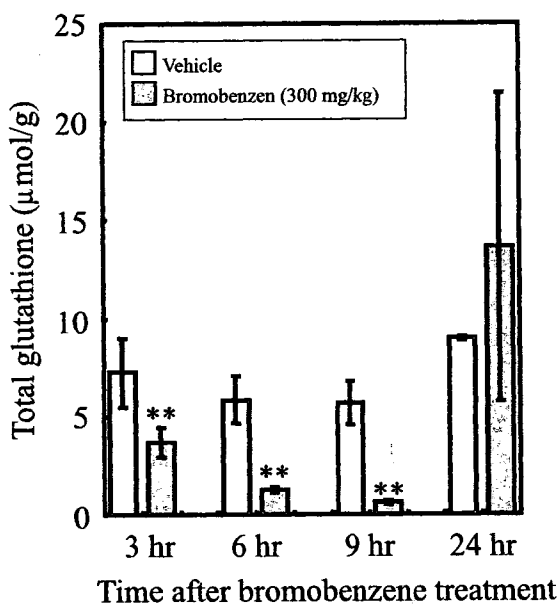

Fig. 5. Glutathione content in rat liver treated with bromobenzene.
Three rats per group were treated with 300 mg/kg bromobenzene or vehicle, and the livers were removed 3, 6, 9 and 24 hr after treatment. Hepatic glutathione content (total) was measured and the data are presented as mean ± S.D. Hepatic glutathione content was significantly decreased 3, 6 and 9 hr after bromobenzene treatment, and recovered 24 hr after treatment, although the glutathione level showed a high variability at this time point. **, $p<0.01$ determined by two-sample *t*-test.

an inverse correlation with hepatic glutathione content.

The present study had two advantages compared with the BSO study previously reported. First, the glutathione-depleting mechanism differs from phorone (a reactor to GSH thiol) and BSO (an inhibitor of gamma-glutamylcysteine synthetase). Comparing the two glutathione-depleting mechanisms, the phorone-induced one is thought to be more similar to drug-induced glutathione depletion (as in the acetaminophen overdose-induced one) where hepatic glutathione is depleted by elevated elimination, not by inhibition of glutathione synthesis. Second, the present study set multiple dose ranges and time points. The total number of rats tested in the phorone study was 36 (twelve 400 mg/kg phorone-treated rats were excluded from the gene selection procedure), whereas the previous BSO study used only 8 rats (Kiyosawa *et al.*, 2004). Thus, the GSH probe sets identified in the present study would give us more reliable information for evaluation of the potential risk of drug-induced glutathione depletion.

The GSH probe sets contained antioxidant/phase II drug-metabolizing enzymes, oxidative stress markers, transporters, metabolism-related genes, transcription factors and signal transduction-related genes, and others. GSH probe sets contain a modifier subunit of glutamate cysteine ligase gene, which encodes a key enzyme for glutathione synthesis (Moinova and Mulcahy, 1999). In addition, a prototypical oxidative stress-responsive gene, heme oxygenase I, which is reported to be regulated by oxidative stress sensor Nrf2 (Nguyen *et al.*, 2003), was identified as GSH probe sets. Furthermore, several genes were found to be in common with previously reported gene sets identified from the BSO-induced glutathione depletion model rat, such as GTP cyclohydrolase I and HMG-CoA reductase (Kiyosawa *et al.*, 2004). On the other hand, a

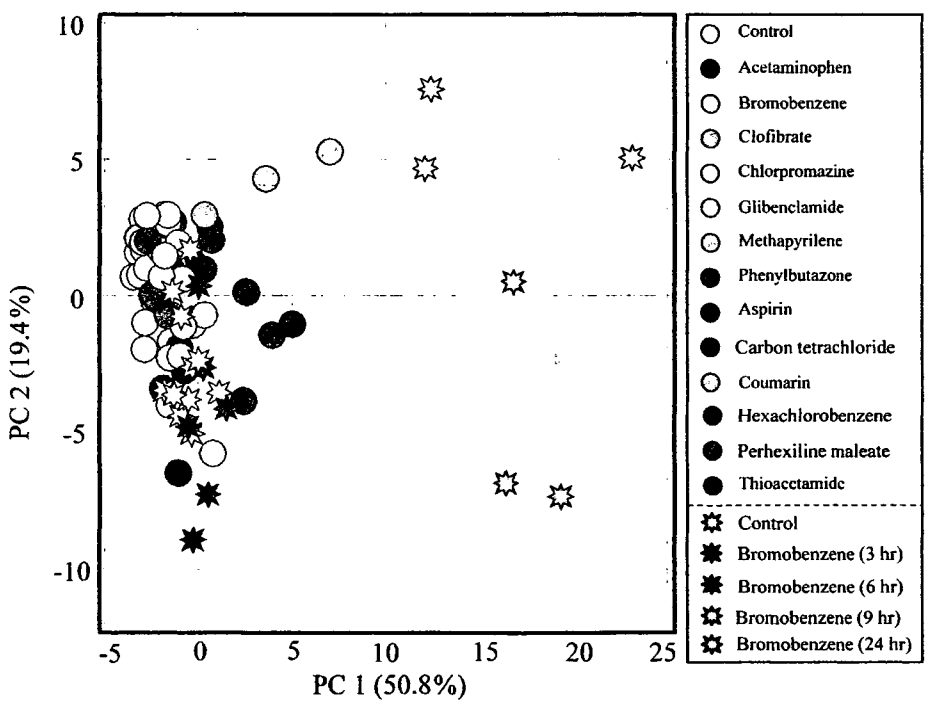

Fig. 6. Time-course of gene expression profile in rat liver treated with bromobenzene.
PCA was performed using GSH probe sets for GeneChip data of rat livers 3, 6, 9 and 24 hr after 300 mg/kg bromobenzene treatment, as well as those 24 hr after treatment with hepatotoxicants, which are the same as those shown in Fig. 4. Each spot colored by chemical types represents individual samples. Gene expression profiles of rats treated with bromobenzene did not show an apparent shift away from corresponding controls 3 and 6 hr after treatment. Those 9 and 24 hr after treatment showed an apparent shift from the controls.

difference in the content of probe sets, compared with that identified from BSO-treated rats was observed, for instance, glutathione *S*-transferase genes or metallothionein genes, which were induced by BSO but not by phorone (Kiyosawa *et al.*, 2004). Although the strain and the age of the rats were not matched between the two studies (6 week old male Crj:CD(SD)IGS rats vs. 9 week old male F344Cu/Drj rats) the difference could be mainly due to the difference of the GSH-depleting mechanism between phorone and BSO.

To examine the toxicological significance of the GSH probe sets, we conducted PCA on GeneChip data obtained from rats treated with 13 prototypical hepatotoxicants (Fig. 4). On the PCA map, rats treated with bromobenzene, coumarin, and acetaminophen showed apparent changes in hepatic gene expression profiles, and those treated with thioacetamide showed slight changes (Fig. 4). Bromobenzene-treated rats showed the most notable change in gene expression. Bromobenzene was reported to be oxidized to a reactive metabolite in liver, depleting hepatic glutathione (Chakrabarti, 1991; Heijne *et al.*, 2004).

Courmarin-treated rats showed the second most affected gene expression profile in PCA. It was reported that a single coumarin treatment reduced the hepatic content of non-protein sulfhydryl groups (Lake *et al.*, 1989), and this is thought to reflect the decrease in glutathione content. Furthermore, coumarin was shown to decrease glutathione content in rat hepatocyte as well (Lake *et al.*, 1989). Reactive metabolites generated from coumarin oxidation in liver were thought to play a role in coumarin-induced glutathione depletion and hepatotoxicity (Lake, 1984; Lake *et al.*, 1989). Since no apparent hepatotoxicity was evident in both the histopathology and plasma biochemistry data (Table 2), the PCA result would reflect the potential risk of courmarin-induced glutathione-depletion.

Acetaminophen and thioacetamide are known to deplete or reduce glutathione in liver when overdosed (Mesa *et al.*, 1996). In the present study, acetaminophen- or thioacetamide treated rat showed no dramatic change in the gene expression profile compared to bromobenzene. Considering the plasma chemistry data, rats treated with acetaminophen or thioacetamide did not show apparent hepatotoxicity within 24 hr after single dose, whereas those treated with bromobenzene apparently showed it, suggesting that glutathione depletion, expression profile of GSH probe sets, and toxicological phenotype are well correlated with each other.

We also investigated the time-course of glutathione content and gene expression profile in rat livers treated with bromobenzene, and this showed the most notable gene expression change of all of the examined hepatotoxicants (according to the PCA result). Bromobenzene rapidly depleted hepatic glutathione 3 hr after treatment, and the glutathione content was the lowest 9 hr after treatment (Fig. 5). Hepatic glutathione content recovered from initial depletion until 24 hr after the bromobenzene treatment, and such recovery has been previously reported (Chakrabarti, 1991; Heijne *et al.*, 2004). On the other hand, gene expression changes had not been apparent 3 and 6 hr after the bromobenzene treatment, but appeared 9 and 24 hr after treatment. Although hepatic glutathione content was recovered at 24 hr after the bromobenzene treatment, a changed level in gene expression was most prominent at this time point. This result depicts a characteristic of the gene expression profile in that it does not reflect the status of hepatic glutathione content itself, but the nuclear activity to maintain glutathione homeostasis in the liver against bromobenzene-induced glutathione depletion. It should be noted, that although the hepatic glutathione content was recovered 24 hr after bromobenzene treatment, the potential risk of bromobenzene-induced glutathione depletion does exist. In general, hepatic glutathione depletion caused by chemical treatments occurs immediately, followed by rapid recovery by glutathione re-synthesis (Meister and Anderson, 1983). Since the time point of sacrifice in ordinal toxicity studies is set to 24 hr after chemical treatment in many cases, measurement of glutathione content might overlook the risk of the glutathione-depleting potential of the tested chemicals, because 24 hr is enough time for the recovery of glutathione content after acute glutathione depletion. Instead, gene expression profiling is considered to be appropriate for evaluating the glutathione-depleting potential of chemicals, rather than measuring glutathione content, especially in later time points of chemical treatment. This characteristic of gene expression profiling, namely toxicogenomics analysis, would allow for safety assessment of chemicals in drug development.

In conclusion, a total of 161 probe sets of RAE 230A GeneChip, referred as GSH probe sets, were identified using phorone-treated rats for evaluation of drug-induced glutathione depletion. The significance of the identified GSH probe sets was evaluated using the TGP database, where prototypical glutathione depletors successfully showed characteristic changes in the signal levels of GSH probe sets. The time-course

of glutathione content and the gene expression profile showed that gene expression profiling could detect the glutathione-depleting potential of chemicals in later time points, e.g., 24 hr after chemical treatment, where hepatic glutathione content had recovered from acute and transient depletion at earlier time points. Therefore, toxicogenomics analysis using identified GSH probe sets would be an invaluable methodology for assessing a drug's potential risk of glutathione depletion, possibly leading to hepatotoxicity.

ACKNOWLEDGMENT

This study was supported in part by a grant from the Ministry of Health, Labor and Welfare (H14-Toxico-001).

REFERENCES

Boverhof, D.R. and Zacharewski, T.R. (2006) : Toxicogenomics in risk assessment: Applications and needs. Toxicol. Sci., **89**, 352-360.

Boyland, E. and Chasseaud, L.F. (1967) : Enzyme-catalysed conjugations of glutathione with unsaturated compounds. Biochem. J., **104**, 95-102.

Chakrabarti, S.(1991): Potential tolerance against bromobenzene-induced acute hepatotoxicity due to prior subchronic exposure. Arch. Toxicol., **65**, 681-684.

Dahlin, D.C., Miwa, G.T., Lu, A.Y. and Nelson, S.D. (1984): *N*-acetyl-*p*-benzoquinone imine: a cytochrome P-450-mediated oxidation product of acetaminophen. Proc. Natl. Acad. Sci. U S A, **81**, 1327-1231.

Heijne, W.H., Slitt, A.L., Van Bladeren, P.J., Groten, J.P., Klaassen, C.D., Stierum, R.H. and Van Ommen, B. (2004): Bromobenzene-Induced Hepatotoxicity at the Transcriptome Level. Toxicol. Sci., **79**, 411-422.

James, L.P., Mayeux, P.R. and Hinson, J.A. (2003): Acetaminophen-induced hepatotoxicity. Drug. Metab. Dispos., **31**, 1499-1506.

Kaplowitz, N.(2004): Drug-induced liver injury. Clin. Infect. Dis., **38**, Suppl. 2, S44-48.

Kiyosawa, N., Ito, K., Sakuma, K., Niino, N., Kanbori, M., Yamoto, T., Manabe, S. and Matsunuma, N. (2004): Evaluation of glutathione deficiency in rat livers by microarray analysis. Biochem. Pharmacol., **68**, 1465-1475.

Lake, B.G. (1984): Investigations into the mechanism of coumarin-induced hepatotoxicity in the rat. Arch. Toxicol., Suppl. **7**, 16-29.

Lake, B.G., Gray, T.J., Evans, J.G., Lewis, D.F., Beamand, J.A. and Hue, K.L. (1989): Studies on the mechanism of coumarin-induced toxicity in rat hepatocytes: Comparison with dihydrocoumarin and other coumarin metabolites. Toxicol. Appl. Pharmacol., **97**, 311-323.

Li, A.P. (2002): A review of the common properties of drugs with idiosyncratic hepatotoxicity and the "multiple determinant hypothesis" for the manifestation of idiosyncratic drug toxicity. Chem. Biol. Interact., **142**, 7-23.

Liu, G., Loraine, A.E., Shigeta, R., Cline, M., Cheng, J., Valmeekam, V., Sun, S., Kulp, D. and Siani-Rose, M.A. (2003): NetAffx: Affymetrix probesets and annotations. Nucleic Acids Res., **31**, 82-86.

Lu, S.C. (1999): Regulation of hepatic glutathione synthesis: Current concepts and controversies. Faseb J., **13**, 1169-1183.

Meister, A. and Anderson, M.E. (1983) Glutathione. Ann. Rev. Biochem., **52**, 711-760.

Mesa, M.L., Carrizosa, R., Martinez-Honduvilla, C., Benito, M. and Fabregat, I. (1996): Changes in rat liver gene expression induced by thioacetamide: Protective role of S-adenosyl-L-methionine by a glutathione-dependent mechanism. Hepatology, **23**, 600-606.

Mitchell, J.R., Jollow, D.J., Potter, W.Z., Gillette, J.R. and Brodie, B.B. (1973): Acetaminophen-induced hepatic necrosis. IV. Protective role of glutathione. J. Pharmacol. Exp. Ther., **187**, 211-217.

Moinova, H.R. and Mulcahy, R.T. (1999): Up-regulation of the human gamma-glutamylcysteine synthetase regulatory subunit gene involves binding of Nrf-2 to an electrophile responsive element. Biochem. Biophys. Res. Commun., **261**, 661-668.

Nguyen, T., Sherratt, P.J. and Pickett, C.B. (2003): Regulatory mechanisms controlling gene expression mediated by the antioxidant response element. Ann. Rev. Pharmacol. Toxicol., **43**, 233-260.

Orphanides, G.(2003): Toxicogenomics: Challenges and opportunities. Toxicol. Lett., **140-141**, 145-148.

Parkinson, A. (2001): Biotransformation of xenobiotics. In (Klaassen, C.D., ed.), pp. 133-224, Casarett and Doull's Toxicology, McGraw-Hill,

New York.

Rockett, J.C. and Dix, D.J. (2000): DNA arrays: Technology, options and toxicological applications. Xenobiotica, **30**, 155-177.

Snedecor, G.W. and Cochran, W.G. (1989): Statistical Methods, 8th ed., Iowa State University Press.

Takashima, K., Mizukawa, Y., Morishita, K., Okuyama, M., Kasahara, T., Toritsuka, N., Miyagishima, T., Nagao, T. and Urushidani, T. (2006): Effect of the difference in vehicles on gene expression in the rat liver-analysis of the control data in the Toxicogenomics Project Database. Life Sci., **78**, 2787-2796.

Urushidani, T. and Nagao, T. (2005): Toxicogenomics: the Japanese initiative. In (Borlak, J., ed.), pp. 623-631, Handbook of Toxicogenomics-Strategies and Applications Wiley-VCH.

van Doorn, R., Leijdekkers, C.M. and Henderson, P.T.(1978): Synergistic effects of phorone on the hepatotoxicity of bromobenzene and paracetamol in mice. Toxicology, **11**, 225-233.

医薬品安全性研究の動向
～マイクロドーズ試験を含めて～

漆谷　徹郎*

ポストゲノム時代，新薬開発は期待に反して加速されていない。ゲノム情報を活用しきれていない段階として安全性研究があるが，この分野もようやく新規技術開発の恩恵を受けるようになってきた。遺伝子型，遺伝子発現，タンパク質，代謝物を網羅的に解析するオミクステクノロジーの進歩は，「何が起こるかわからない毒性」を予測するための手がかりを与えてくれる。安全性研究者は，これらを臨床開発にまで利用できるバイオマーカーへと発展させる義務を負うが，それには多くの困難を克服する必要がある。マイクロドーズ試験は臨床治験を加速する手段として期待されているが，少なくともわが国の現状では安全性研究にインパクトを与えるには至っていない。

■キーワード：オミクステクノロジー，トキシコゲノミクス，バイオマーカー，マイクロドージング，早期探索的臨床試験

1 はじめに

ポストゲノム時代に入り，医薬品開発は新たな局面を迎えている。ヒトゲノムプロジェクトの進行中，ゲノム配列は宝の山であるという過大な期待が寄せられていたが，現在その熱は冷めつつある――というより，現実的な扱いになってきた。主要な医薬品としてGPCR（Gタンパク質共役型受容体）をターゲットとするものが多いことから，GPCR様配列がゲノム上に多数見出されたとき，新規医薬品開発を夢みた研究者は多かったが，そのほとんどは嗅覚受容体であることが判明し，期待はずれに終わった。しかしそうはいっても，遺伝性疾患の原因遺伝子に基づく薬物のターゲット策定や作用メカニズム解析において，ゲノム情報の寄与は大きい。毎週のように疾患関連遺伝子を同定したとの報道がなされ，それらの記事は「今回の発見は治療薬の開発につながる」と結ばれるのが常である。これが事実なら多くの難治性疾患があっという間に克服されるはずであるが，画期的な新薬が登場する数は年々減少の一途にある。

図1はしばしば引用される開発中止を余儀なくされた薬物の中止理由の変遷である。対外発表の場合必ずしも実情を反映していない場合があるにしても，特に減少が目立つのが薬物動態関連である。これは，その少なくとも一部にヒト型の薬物代謝酵素やトランスポーターの利用による予測性向上，すなわちヒトゲノム情報が寄与しているに違いない。一方，相対的に毒性関連の理由が増えており，さらに「有効性」を「安全性を考えるとそれ以上増量できないために目的の有効性が達成で

*同志社女子大学薬学部 医療薬学科病態生理学研究室　教授（うるしだに・てつろう）
（独）医薬基盤研究所 トキシコゲノミクス・インフォマティクス プロジェクトリーダー

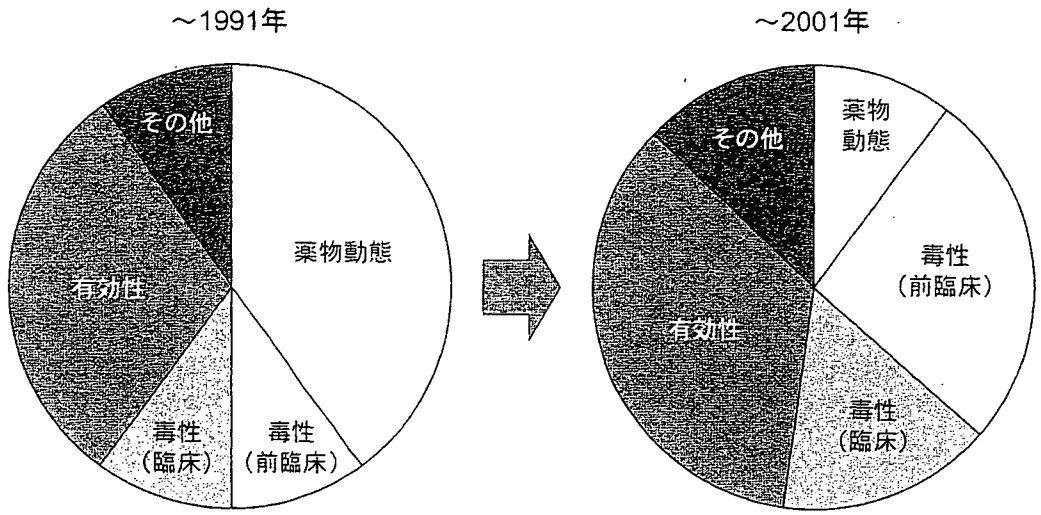

図1 米国における医薬品の開発中止理由の変遷
1991年の統計と，2001年の統計の比較で，この10年間に薬物動態を理由とするものが大幅に減った。
(Nature Rev. Drug Discov. 3：711-715 (2004) に記載のデータに基づき，筆者が改変)

きない」と考えると，ほとんどの理由が安全性関連と考えても差し支えないであろう。すなわち，安全性研究はまだゲノム情報解明の恩恵が薄いため，創薬プロセスから取り残された領域といえる。しかしながら，この分野にも着実な進歩の波が押し寄せている。

2 オミクステクノロジー

薬物開発の各段階，有効性の検討はターゲットが絞られている分，最新技術の応用がしやすい。一方，薬理作用の延長上にない範疇の毒性に関しては予めその対象を絞ることができない。サリドマイドの例を出すまでもなく，臨床で問題になった後にその有害作用を動物実験で再現することすら，かなりの努力を要するが，それを全く白紙の状態から予測しなければならない。薬物が生体に与える影響をすべて観測する方法があって初めて出発点に立てるのであるが，そんなことは不可能であると前世紀までの毒性学者は考えていたであろう。しかし，それに近いことを実現する技術，オミクステクノロジー (omics technology) が開発されてきたのである。

～ome とは「全体」を表す語尾，～ics とは「学問」を表す語尾であり，～omics とは「全体を扱う学問」ということになる。すなわち遺伝子全体(或いは発現遺伝子全体)，タンパク質全体，代謝物全体を網羅的に解析するものを，それぞれゲノミクス(genomics)，プロテオミクス(proteomics)，メタボロミクス (metabolomics) と呼び，これら技術を毒性学に適用した場合を，それぞれにトキシコ (toxico) という接頭語をつけて呼ぶ。

DNA マイクロアレイ技術の開発によって可能となったトキシコゲノミクス (toxicogenomics) には二つの方向性がある。ひとつは，遺伝子型と疾患，薬物代謝，薬物感受性などとの関連を見出すことによって，個別医療の道を開くことである。これは当然臨床の安全性確保にもつながることが期待される。個人の遺伝子型を決定するにはまだコストがかかるが，将来は，個々の患者がCYP の SNPs などの情報が入った IC チップを所持する時代が来るのであろうか。現在の段階では，個人差の大きい薬物代謝酵素には影響されないタイプの化合物を選択する，という戦略が主である。もう一つは，薬物投与後に生じる毒性学的変化を遺伝子発現の変化として捉えるものである。(mRNA の発現量の網羅的解析＝トランスクリプトミクス〔transcriptomics〕と呼ぶべきであるが，この語はあまり一般的でない)。非臨床安全

性研究において最も有効な使い道は，多種の既存薬物を投与した動物の各臓器における網羅的遺伝子発現変動をデータベースとして蓄えておき，開発候補品のそれと比較することにより毒性予測をするというものである。古典的毒性学的パラメーターの評価に比べて感度が高く，また毒性メカニズムに関しても同時に情報が得られることから，有用な方法である。ただし，予測性を高めるためには多量かつ均一なデータを蓄積する必要があり，これには膨大なコストがかかるため，欧米の巨大製薬企業でないと自前のデータベースをもつことはなかなか困難である。そこでわが国では，筆者も関係している，官民共同の「トキシコゲノミクスプロジェクト」が2002(平成14)年度から5年計画で行われ[1]，現在は第2期目「トキシコゲノミクス・インフォマティクスプロジェクト」に入っている。

トランスクリプトミクスの問題点として，

① 重要な遺伝子群が抽出されても，臨床に応用する場合バイオプシーが必要となり，現実的でない。
② たとえ毒性学的メカニズムが共通でも，個々の遺伝子発現でみると種差が大きい場合がある。
③ 翻訳後修飾が毒性学的に重要である場合が多く，mRNA量が直接機能と相関しない場合が多い。

などが挙げられる。種差を克服する手段としては，直接ヒトサンプルを対象にするのが理想であるが，バイオプシーが非現実的な選択である場合，遺伝子発現解析が可能な臨床サンプルとしては末梢血がほぼ唯一のものである。まだ成功例は少ないが，予測可能であるとの報告があり[2]，上記プロジェクトにおいてもデータ収集を開始している。

毒性学的機能に直結した因子を観測するには，タンパク質や代謝物の網羅的解析が必要となる。検出時に増幅が可能な遺伝子と異なり，特にタンパク質の検出感度は低い。現在，2D-DIGE（対照群と処置群を別々の蛍光色素でラベルしたものを混合し，2次元電気泳動で分離して，色調の変化で量の変動を定量する）で検出したタンパク質を質量分析で同定する方法が，最も効率がよいが，スループット性は低い。さらに，標的臓器において重要なマーカータンパク質が同定されても，これが臨床的に利用可能な侵襲度の低いサンプルに反映される確率は低いという，mRNA量と同様の問題がある。もちろん，他の方法で推定されたメカニズムの検証には，大いに利用価値があろう。

一方，低分子代謝物を検出するメタボロミクスは，高速液体クロマトグラフィーで分離後質量分析にかける方法と，核磁気共鳴スペクトルのピーク変化をデータベース化する方法に大別される。両方法とも，血清や尿という臨床に直結するサンプルに適応可能であるという大きな利点をもっている。その反面，変化する対象の同定が困難であり，必然的に毒性メカニズムに結び付け難いという問題が生じる。

結局，網羅的解析omicsといっても，複雑な生理反応に伴う変化のある一部を切り取ったものに過ぎず，それだけですべてを記述することには無理がある。そこで各網羅的解析結果を統合して解析する立場，トキシコパノミクス(toxicopanomics)の必要性が唱えられている。これは，安全性研究に限ったことではなく，すべての生命科学分野に当てはまることである。今世紀，重点的に発展させていく必要のある領域として，システムズバイオロジー(systems biology)が注目されているゆえんである。

3 バイオマーカーとレギュラトリーサイエンス

バイオロジストたるもの，客観的な指標なしに研究はできないのであり，バイオマーカーの概念は以前から存在していた。NIH（米国国立衛生研究所）の定義によれば，「客観的に測定され，評価される特性値であり，正常な生物学的プロセス，病理学的プロセス，または治療処置に対する薬理学的反応の指標として用いられるもの」であり，薬物開発に欠かせないことはいうまでもない。しかし創薬研究においてバイオマーカーという単語が注目されたのは，米国FDA（食品医薬品局）が明確な定義を発表してからである。「測定できる特性値であり，ヒトまたは動物における生理学的プロセス，薬理学的プロセス，または疾病プロセス

を反映しているもの。治療に伴うバイオマーカーの変化は当該製品に対する臨床的反応を反映する」という定義は，内容的には大差ないと感じられるが，薬物開発におけるインパクトは大きかった。その立場は2004年3月にFDAが発表したレポート「クリティカルパス・イニシアチブ(CPI: Critical Path Initiative)」(真に有効で安全な新規医薬品をいち早く患者に提供するために，産・官・学が協力して従来の開発プロセスを見直そうという構想)で明らかとなる[3]。CPIについては他稿に譲るが，「医薬品の開発が遅れているのは先端技術の取り入れが甘い段階があるためである。最新技術を取り入れ，薬剤開発に当たっては基礎研究から市販後に至るまで利用可能なバイオマーカーを確立する努力をせよ」という，規制側から突きつけられた要求と解釈できよう。もちろん，基礎研究用のローカルなバイオマーカーはそれなりに利用価値がある。しかし，次のような例を考えてみよう。ある生活習慣病の治療薬を開発している。長期連用したラットの肝臓で，ある遺伝子Xの発現変化が起き，無視できない有害作用につながる可能性が示唆されているが，ヒトでこれが起こるかどうかは不明である。連続的にバイオプシーをして有害作用発現前に遺伝子変化を捉えることができれば治験で評価できるが，生活習慣病のために何度も肝臓のバイオプシーを施行するのは現実的でない。ここでの遺伝子Xは立派なバイオマーカーであるが，臨床に適応できず，臨床開発において無力である。ここで安全性研究者に求められているのは，「ラットの肝臓における遺伝子X」を知ってしまった以上，この薬物を臨床開発するための安全性バイオマーカーを開発する義務を負う，ということである。

この狭義でのバイオマーカーの開発は，がん治療の領域，特に分子標的薬の分野での進歩が著しい。バイオマーカーは，診断マーカーと患者選別マーカーに分けられる。診断マーカーは（抗体のように病因が消失したのちも存続するものもあるが）多くの場合，薬効を判定するマーカーともなりうる。患者選別マーカーは，特定の医薬品が奏効する患者群を選別する目的で用いられ，例えば特定の遺伝子変異を標的とする抗がん剤の場合などに威力を発揮する。がんの場合，適正な治療方針を決定するのが急務であること，無効な抗がん剤の使用は有害作用が大きいこと，患部のバイオプシーを行う科学的・倫理的理由がみたされることなど，ゲノム情報を活用した生物学的裏付けのある臨床利用可能なバイオマーカー開発に適した環境にある。現在安全性研究者に求められているのは，非臨床で得られる科学的知識を，臨床で評価可能な具体的な指標として提示することなのである。

4 マイクロドージング

臨床開発の各段階における臨床試験デザインとその目的については，これまでの紆余曲折を経ながら「臨床試験の一般指針」に示されている。しかし最近，欧米の規制当局は第Ⅰ相試験よりも前の前臨床開発の過程で，ヒトを対象とした探索的な臨床試験(早期探索的臨床試験)の導入を推進している[4]。

早期探索的臨床試験は，投与用量をヒトに有害作用が現れないと想定される用量以下，投与期間を短期に限定して行うものである。医薬品開発の初期段階で医薬品候補物質の絞り込みや開発可否の見極めが目的であり，診断や治療を目的とするものではない。通常の第Ⅰ相試験で行われる最大耐量を求めることも意図していないことから，これを実施するために必要な非臨床安全性試験は，通常よりも規模や用量，方法を縮小・簡略化できる。従って，目的は限定されるが，従来よりも早期に臨床試験を実施できるという利点があるとされる。

早期探索的臨床試験で得ることが期待されている情報としては，

① ヒトでの薬物動態情報
② ヒト体内分布に関する情報
③ *in vivo* あるいは *in vitro* の薬効スクリーニング系から期待される薬効がヒトでも得られるかに関する情報
④ 薬効に関連するバイオマーカーに関する情報

などがある。早期探索的臨床試験はその臨床投与量に基づき，(1)極めて低い用量を用いて薬物動態を検討する「マイクロドーズ臨床試験」，(2)